^{61}Cu(^{61}Ni) emission Mossbauer study of hyperfine interactions in copper-based oxides

1995 J. Phys.: Condens. Matter 7 2339

(http://iopscience.iop.org/0953-8984/7/11/012)

J. Phys.: Condens. Matter 7 (1995) 2339–2344. Printed in the UK

^{61}Cu(^{61}Ni) emission Mössbauer study of hyperfine interactions in copper-based oxides

F S Nasredinov, P P Seregin, V F Masterov, N P Seregin, O A Prikhodko and M A Sagatov

St Petersburg State Technical University, 195251, St Petersburg, Russia

Received 30 September 1994

Abstract. Simple (CuO_2, CuO) and complex superconducting ($YBa_2Cu_3O_{7-x}$, $La_{2-x}Sr_xCuO_4$) copper oxides have been investigated by ^{61}Cu(^{61}Ni) emission Mössbauer spectroscopy. A linear relationship between the quadrupole coupling constant for ^{61}Ni and the calculated lattice electric field gradients is established, and the contribution of the Ni^{2+} valence electrons to the coupling constant is determined. Magnetic fields are observed at ^{61}Ni nuclei in those cases when the copper sublattice shows magnetic ordering.

1. Introduction

Mössbauer spectroscopy with various isotopes (^{57}Fe, ^{119}Sn, ^{151}Eu, ^{155}Gd, ^{161}Dy, ^{170}Yb) has been widely used for investigating copper based HTSCs. Such investigations are of particular interest in those cases when the Mössbauer probe resides at the copper sites. For this reason we have developed and applied to $YBa_2Cu_3O_{7-x}$ [1] and $La_{2-x}Sr_xCuO_4$ [3] ^{67}Cu(^{67}Zn) emission Mössbauer spectroscopy. In this technique the $^{67}Zn^{2+}$ probe is produced at a copper site by decay of a ^{67}Cu parent nucleus, and the nuclear and atomic parameters of the probe allow one to determine all the parameters of the tensor of the electric field gradient (EFG) created at the copper sites by the lattice ions. However, ^{67}Zn Mössbauer spectra could not be observed for sites with magnetic ordering because of certain technical obstacles. To investigate the combined magnetic and electric quadrupole interactions of the nuclei at the copper sites of the HTSC lattices we have proposed ^{61}Cu(^{61}Ni) emission Mössbauer spectroscopy [3]. In this case the $^{61}Ni^{2+}$ Mössbauer probe produced by decay of ^{61}Cu also occupies a copper site. In addition, the nuclear and atomic parameters of the probe are suitable for both the magnetic and electric quadrupole interactions to be observed. The present paper reports ^{61}Cu(^{61}Ni) emission Mössbauer data for typical HTSCs, $YBa_2Cu_3O_{7-x}$ and $La_{2-x}Sr_xCuO_4$, as well as for simple copper oxides, Cu_2O and CuO.

2. Experimental details

Ceramic samples of $YBa_2Cu_3O_{7-x}$ ($x = 0$ or 1) and $La_{2-x}Sr_xCuO_4$ ($x = 0$ or 0.15) were prepared by sintering the corresponding oxides. The homogeneity of the samples was controlled by x-ray diffraction. T_c values of 91 and 40 K were found for $YBa_2Cu_3O_7$ and $La_{1.85}Sr_{0.15}CuO_4$, respectively. Cu_2O and CuO samples were prepared by decomposing cupric nitrate in air.

0953-8984/95/112339+06$19.50

The ^{61}Cu isotope was produced by the ^{61}Ni(p,n)^{61}Cu reaction followed by chromatographic isolation of a carrier-free $^{57}CuCl_2$ preparation. Radioactive copper was introduced into $YBa_2Cu_3O_{7-x}$ or $La_{2-x}Sr_xCuO_4$ samples by thermal diffusion, which ensures that the radioactive copper atoms occupy regular copper sites [4]. The doping of Cu_2O and CuO with radioactive copper was effected through the starting copper nitrate.

The Mössbauer spectra were recorded on a commercial spectrometer at 80 K. The $Ni_{0.86}V_{0.14}$ alloy with a surface density of 1500 mg cm^{-2} was used as a standard absorber. Each spectrum was, as a rule, recorded on four to six samples.

3. Experimental results and discussion

As reported earlier [5], the appearance of an isomer shift in ^{61}Ni Mössbauer spectra is unlikely. Experimental spectra may reveal only the effects of electric quadrupole and Zeeman interactions of the ^{61}Ni nuclei with local fields. A purely quadrupole interaction splits the ground and excited levels of ^{61}Ni nuclei into two and three sublevels, respectively, so that the Mössbauer spectrum is a superposition of five lines whose intensities relate as 10:4:1:6:9. A purely Zeeman interaction splits the Mössbauer spectrum into 12 symmetrical lines whose intensities relate as 10:4:1:6:6:3:3:6:6:1:4:10. In the case of combined hyperfine interaction the eigenvalues of the Hamiltonian for an axially symmetrical EFG tensor and $eQU_{zz} \ll gH$ are given by

$$E_m^I = mgH + \frac{eQU_{zz}}{4I(2I-1)}[3m^2 - I(I+1)]\frac{3\cos^2\theta - 1}{2} \tag{1}$$

where H and U_{zz} are the magnetic field and the principal component of the EFG tensor (both at the nucleus), θ is the angle between the direction of the magnetic field and the z-axis of the EFG tensor, m is the magnetic quantum number; I and Q are the spin and the quadrupole moment of the nucleus, respectively, and g is the gyromagnetic ratio. For ^{61}Ni the last three quantities are: $I_0 = \frac{3}{2}$, $Q_0 = 0.162$ b, $g_0 = -0.701$ mm s^{-1} T^{-1} in the ground state and $I_e = \frac{5}{2}$, $Q_e = -0.2$ b, $g_e = 0.0268$ mm s^{-1} T^{-1} in the excited state [6]. The quadrupole coupling constants given below relate to the ground state of ^{61}Ni.

Spectra of simple copper oxides, Cu_2O and CuO, are of particular interest for substantiating the potentialities of ^{61}Cu(^{61}Ni) emission Mössbauer spectroscopy in studying copper-based HTSCs. In both the oxides copper atoms occupy only one crystallographic position, the symmetry of the copper environment being non-cubic, and, therefore, appearance of quadrupole splitting in the spectra is to be expected. However, as figure 1(*a*) shows, the $^{61}Cu_2O$ spectrum is a somewhat broadened singlet for which only the upper limit for the quadrupole coupling constant, $|eQ_0U_{zz}| < 30$ MHz, could be found. For Ni^{2+} ions the EFG at ^{61}Ni nuclei is created by lattice ions (lattice EFG), as well as by the non-spherical valence shell of the Ni^{2+} ions themselves (valence EFG), so that

$$U_{zz} = (1-\gamma)V_{zz} + (1-R_0)W_{zz} \tag{2}$$

where U_{zz}, V_{zz}, W_{zz} are the principal components of the total, lattice and valence EFGs, respectively; γ and R_0 are the Sternheimer factors for Ni^{2+}. The lattice EFG tensor may be calculated in the point charge approximation, and calculations for the $Cu_2^+O^{2-}$ model, carried out with the use of x-ray data [7], give $V_{zz} = -1.09$ e Å^{-3} at the copper sites. For $\gamma = -7.92$ [8] the above value of V_{zz} results in $eQ_0V_{zz}(1-\gamma) = -55$ MHz, which

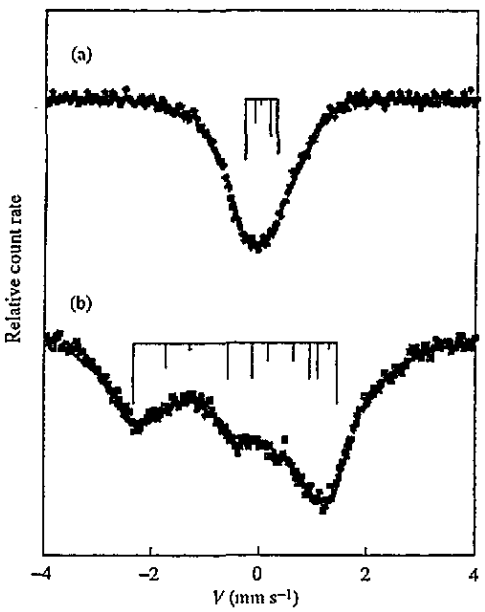

Figure 1. $^{61}Cu(^{61}Ni)$ emission Mössbauer spectra of (*a*) Cu_2O and (*b*) CuO. The positions of the components of (*a*) the quadrupole and (*b*) Zeeman multiplets are shown.

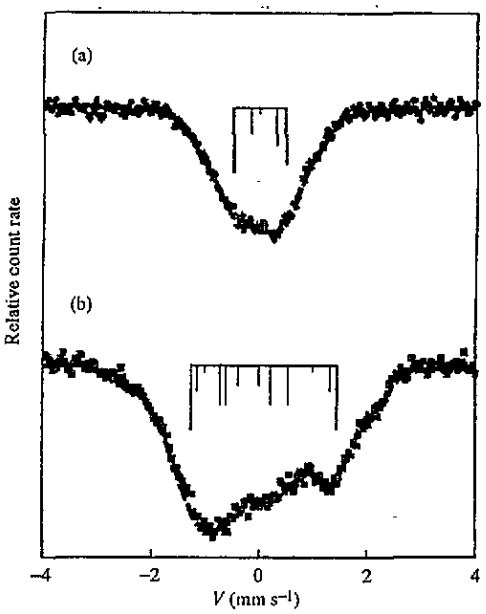

Figure 2. $^{61}Cu(^{61}Ni)$ emission Mössbauer spectra of (*a*) $La_{1.85}Sr_{0.15}CuO_4$ and (*b*) La_2CuO_4 ceramic samples. The positions of the components of (*a*) the quadrupole and (*b*) Zeeman multiplets are shown.

much exceeds the experimental value. This discrepancy is obviously caused by the valence contribution to the EFG for Ni^{2+} ions. If the terms $(1-\gamma)V_{zz}$ and $(1-R_0)$ in equation (2) are nearly equal in magnitude and opposite in sign, then these contributions compensate each other, and the total EFG is substantially decreased.

Such compensation is not so effective for the CuO matrix, as indicated by the spectrum in figure 1(*b*) for which $eQ_0U_{zz} = -43 \pm 2$ MHz, whereas calculation of the EFG for the $Cu^{2+}O^{2-}$ model with the use of x-ray data [9] gives $eQ_0V_{zz}(1-\gamma) = 37$ MHz. This means that the valence contribution of Ni^{2+} to the total EFG may be estimated as $eQ_0W_{zz}(1-R_0) = -80$ MHz. The spectrum in figure 1(*b*) reflects the combined magnetic and electric quadrupole interaction of ^{61}Ni with the local fields in accordance with the antiferromagnetism exhibited by CuO below 230 K. The fine structure of the spectrum corresponds to an effective magnetic field $H = 11.5 \pm 0.5$ T; the eQ_0U_{zz} value is estimated for $\theta = 0°$ (according to [10], $\theta < 10°$).

Copper atoms occupy in the $La_{2-x}Sr_xCuO_4$ lattice only one crystallographic position with a non-cubic environment. At $x < 0.08$ the copper sublattice shows antiferromagnetic ordering with the highest Néel temperature $T_N = 250$ K at $x = 0$ [10]. The $^{61}Cu(^{61}Ni)$ emission Mössbauer spectrum of a superconducting $La_{1.85}Sr_{0.15}CuO_4$ sample (figure 2(*a*)) is a poorly resolved quadrupole multiplet with $eQ_0U_{zz} = -50 \pm 2$ MHz, whereas that of a non-superconducting La_2CuO_4 sample (figure 2(*b*)) shows combined hyperfine interaction ($H = 8.5 \pm 0.5$ T and $eQ_0U_{zz} = -45 \pm 2$ MHz if $\theta = 80°$ is assumed, according to [10]). These results show that the EFG at the copper sites does not change considerably in going from La_2CuO_4 to $La_{1.85}Sr_{0.15}CuO_4$, which is in good agreement with ^{63}Cu NMR data for $La_{2-x}Sr_xCuO_4$ [10, 11], as well as with our calculations of the

lattice EFG resulting in V_{zz} values of 0.588 and 0.604 e Å^{-3} for the $La^{3+}Cu^{2+}O^{2-}$ and $La^{3+}_{1.85}Sr^{2+}_{0.15}Cu^{2+}O(1)^{2-}_{2}O(2)^{1.925-}_{2}$ models, respectively. These calculations used structural data of [12] and a charge distribution proposed in [2]. Here, O(1) and O(2) denote the oxygen ions lying in the La(Sr)–O and Cu–O planes, respectively.

When the material under investigation has more than one structural state of copper, the interpretation of experimental spectra becomes complicated, since the spectra are, as a rule, unresolved. However, determination of parameters of both the magnetic and quadrupole interactions is possible in this case, too. A typical example is $YBa_2Cu_3O_{7-x}$ where copper occupies two positions, Cu(1) and Cu(2), whose populations relate as 1:2. The $^{61}Cu(^{61}Ni)$ emission Mössbauer spectrum of superconducting $YBa_2Cu_3O_7$ ceramics (figure 3(*a*)) is a superposition of two quadrupole multiplets with eQ_0U_{zz} values of -54 ± 2 and -35 ± 2 MHz. Their relative intensities indicate that these multiplets should be assigned to Ni^{2+} at the Cu(1) and Cu(2) sites, respectively. In non-superconducting $YBa_2Cu_3O_6$ the Cu(2) sublattice is magnetically ordered below 500 K [13]. For this reason the $^{61}Cu(^{61}Ni)$ emission Mössbauer spectrum of this ceramic (figure 3(*b*)) is to be considered as a superposition of two components corresponding to the Cu(2) and Cu(1) sites, respectively, a singlet with $|eQ_0U_{zz}| < 20$ MHz and a magnetic multiplet with $H = 8.5 \pm 0.5$ T and $eQ_0U_{zz} = -48 \pm 2$ MHz; here $\theta = 90°$ is assumed for Cu(2), according to [16].

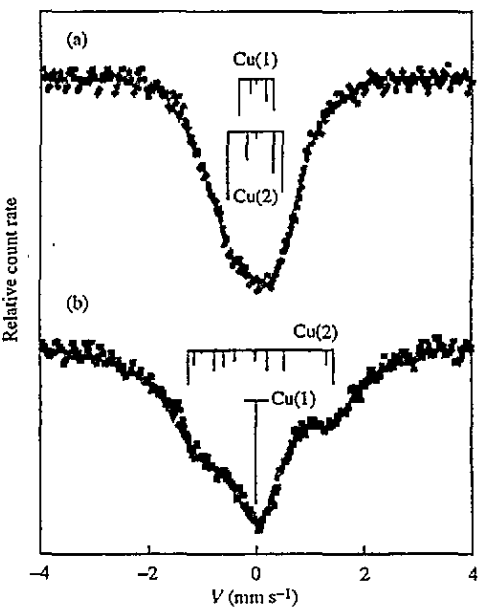

Figure 3. $^{61}Cu(^{61}Ni)$ emission Mössbauer spectra of (*a*) $YBa_2Cu_3O_7$ and (*b*) $YBa_2Cu_3O_6$. Two quadrupole multiplets corresponding to $^{61}Ni^{2+}$ at the Cu(1) and Cu(2) sites are shown in spectrum (*a*). The Zeeman multiplet from the Cu(2) sites and the singlet from the Cu(1) sites are shown in spectrum (*b*).

The parameters of the above spectra and the results of calculations of the lattice EFG tensor are presented in figure 4(*a*) as a plot of $|eQ_0U_{zz}|$ against $|V_{zz}|$. The EFG calculation procedure for Cu_2O, CuO and $La_{2-x}Sr_xCuO_4$ is described above. The EFG tensor was calculated for the $Y^{3+}Ba^{2.06+}_{2}Cu(1)^{1.96+}Cu(2)^{2.01+}_{2}O(1)^{2.13-}_{2}O(2)^{1.95-}_{2}O(3)^{1.84-}_{2}O(4)^{1.26-}$

model (here O(1) is the apical oxygen, O(2) and O(3) are the plane oxygens, O(4) is the chain oxygen) with the use of structural data [14] and of a charge distribution with a hole at O(4), proposed in [14], to give V_{zz} values of 0.949 and 0.566 for the Cu(1) and Cu(2) sites, respectively. Similar calculations for $YBa_2Cu_3O_6$ using structural data of [16] and a simple charge distribution model, $Y^{3+}Ba_2^{2+}Cu(1)^{+}Cu(2)_2^{2+}O_6^{2-}$ [1], give $V_{zz} = -1.253$ and 0.666 e Å^{-3} for the Cu(1) and Cu(2) sites, respectively.

Figure 4(*a*) shows that the data presented are satisfactorily fitted by a straight line. Most points in figure 4(*a*) correspond to $eQ_0U_{zz} < 0$ and $V_{zz} > 0$. For these points the plot $|C_{Ni}|$ against $|V_{zz}|$ is equivalent to the plot in the natural axis (eQ_0U_{zz}) against V_{zz} which is clearly explained with equation (2). But the points 1 and 7 having large negative V_{zz} value and small eQ_0U_{zz} values with uncertain signs are close to the straight line, too. This means that such a choice of axes places the points from the opposite quadrant in the natural axes at the main plot. Thus, the C_{Ni} against $|V_{zz}|$ plot demonstrates more clearly a common kind of dependence of the quadrupole coupling constant on the lattice EFG for both positive and negative V_{zz} values. According to equation (2) the observed linear dependence points to a constant valence contribution $|eQ_0(1-R_0)W_{zz}|_{Ni}$ to the quadrupole coupling constant. An extrapolation of the straight line to $V_{zz} = 0$ gives $|(1-R_0)eQ_0W_{zz}|_{Ni} = 78 \pm 10$ MHz. The negative slope of the straight line evidences opposite signs of the valence and lattice contributions to the EFG. The value of the slope, 56 MHz e^{-1} Å^3, allows one to find the Ni^{+2} Sternheimer factor, $\gamma = -9 \pm 1$, which is quite close to the calculated value $\gamma = -7.92$ [8].

The same valence EFG for all the Ni states studied is somewhat surprising since the environment of the Ni^{+2} ions varies considerably. It is especially surprising that the positive $(1-R_0)eQ_0W_{zz}$ value for Ni^{+2} in Cu_2O and in Cu(1) sites of $YBa_2Cu_3O_6$ (points 1 and 7, respectively) and the negative one for Ni^{+2} in the other matrices have the same magnitudes. There is no clear explanation for this coincidence but it should be marked.

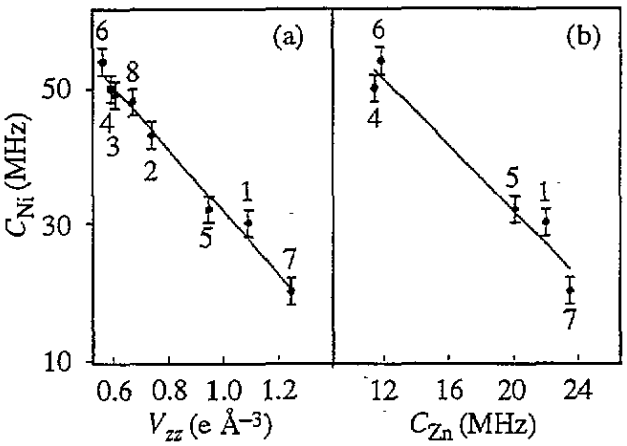

Figure 4. (*a*) $|C_{(Ni)}|$ against $|V_{zz}|$ and (*b*) $|C_{(Ni)}|$ against $|C_{(Zn)}|$ plots for various matrices: Cu_2O (1); CuO (2); La_2CuO_4 (3); $La_{1.85}Sr_{0.15}CuO_4$ (4); Cu(1) in $YBa_2Cu_3O_7$ (5); Cu(2) in $YBa_2Cu_3O_7$ (6); Cu(1) in $YBa_2Cu_3O_6$ (7) and Cu(2) in $YBa_2Cu_3O_6$ (8).

Figure 4(*b*) shows a correlation between the quadrupole coupling constants $|C_{Ni}| = |eQ_0U_{zz}|_{Ni}$ and $|C_{Zn}| = |eQU_{zz}|_{Zn}$ derived from the $^{61}Cu(^{61}Ni)$ and $^{67}Cu(^{67}Zn)$ Mössbauer spectra, respectively. This plot is similar to that in figure 4(*a*) because $(eQU_{zz})_{Zn} \sim V_{zz}$

as shown in [1–4, 15]. The reasons for plotting $|eQ_0U_{zz}|_{Ni}$ against $|eQU_{zz}|_{Zn}$ rather than $(eQ_0U_{zz})_{Ni}$ against $(eQU_{zz})_{Zn}$ are the same as for figure 4(*a*).

While the number of experimental points in figure 4(*b*) is less than that in figure 4(*a*), as $^{67}Cu(^{67}Zn)$ data are scarce, figure 4(*b*) involves no ambiguity in choosing a model for calculating V_{zz}. An extrapolation of the straight line in figure 4(*b*) to $|C_{Zn}| = 0$ gives $|(1-R_0)eQ_0W_{zz}|_{Ni} = 80\pm12$ MHz, which coincides with the value derived from figure 4(*a*) within error. The slope of the plot in figure 4(*b*) also evidences the opposite signs of $(1-R_0)eQ_0W_{zz}$ and $(1-\gamma)eQ_0V_{zz}$.

4. Conclusions

We have considered the use of the $^{61}Cu(^{61}Ni)$ isotope as a Mössbauer probe for studying hyperfine interactions at copper sites of the HTSC lattices. Like other Mössbauer probes, this one allows the EFG tensor parameters at the Cu sites to be determined. In contrast to $^{67}Zn^{2+}$, the $^{61}Ni^{2+}$ probe shows a considerable valence contribution to the EFG. A correlation has been found between the ^{61}Ni quadrupole coupling constant and the lattice EFG at Cu sites. The valence contribution to the ^{61}Ni coupling constant has been determined. The magnetic fields at the Cu sites of the HTSC and related materials have been shown to be detectable by $^{61}Cu(^{61}Ni)$ emission Mössbauer spectroscopy.

Acknowledgment

This work was supported by the Russian Scientific Council on High-Temperature Superconductivity, grant No 91139 'Resonance'.

References

[1] Seregin N P, Nasredinov F S, Masterov V F and Daribaeva G T 1991 *Supercond. Sci. Technol.* **4** 263
[2] Seregin N P, Masterov V F, Nasredinov F S, Saidov Ch S and Seregin P P 1992 *Supercond. Sci. Technol.* **5** 675
[3] Masterov V F, Nasredinov F S, Saidov Ch S, Seregin P P, Bondarevskiy S I and Shchrbatyuk O K 1992 *Superconductivity (KIAE)* **5** 1339
[4] Masterov V F, Nasredinov F S, Saidov Ch S, Seregin P P and Shchrbatyuk O K 1992 *Sov. Phys.–Solid State* **34** 1228
[5] Love J C, Obenshain F E and Czjzek G 1971 *Phys. Rev.* B **3** 2837
[6] *Mössbauer Effect Data Center Information Services and Activities 1985* (Carolina: University of Nortz) p 40
[7] Wells A F 1984 *Structural Inorganic Chemistry* 5th edn (Oxford: Clarendon) p 1120
[8] Gupta R P and Sen S K 1973 *Phys. Rev.* B **8** 1169
[9] Asbrink S and Narrby L J 1970 *Acta Crystallogr.* B **26** 8
[10] Tsudo T, Shimizu T, Yasuoka H, Kishio K and Kitazawa K 1988 *J. Phys. Soc. Japan* **57** 2908
[11] Ohsugi S, Kitaoka Y, Ishida K and Asayama K *J. Phys. Soc. Japan* **60** 2351
[12] Tarascon J M, Grene L H, McKinnen W R, Hull G W and Geballe T H 1987 *Science* **235** 1373
[13] Yasuoka H, Shimizu T, Imai T, Sasaki S, Ueda Y and Kosuge K 1989 *Hyperfine Interact.* **49** 167
[14] Francois M, Jund A, Yvon K, Hewat A W, Capponi J J, Strobel P, Marezio M and Fischer P 1988 *Solid State Commun.* **66** 1117
[15] Masterov V F, Nasredinov F S, Seregin N P and Seregin P P 1992 *Superconductivity (KIAE)* **5** 1830
[16] Yvon K and Francois M 1989 *Z. Phys.* B **76** 413